The Multivariable Control of Carbon Dioxide Absorption System using the Proportional Integral Plus (PIP) Controller

Fereshte Tavakoli Dastjerd[a], Jafar Sadeghi[a],*

Department of Chemical Engineering, Faculty of Engineering, University of Sistan and Baluchestan, Zahedan, Iran

Abstract

The present article investigates the multivariable control of the carbon dioxide absorption process of the Shiraz petrochemical ammonia unit using the proportional-integral-plus (PIP) controller without limitation on the number of controlled variables. The PIP controller is a rational extension of conventional PI/PID controllers with extra dynamic feedback and input compensators. A multi-input – multi-output (MIMO) square model was extracted from the step response test. In this way, input water flow rate to carbon dioxide absorption system, the heat duty of input absorbent cooler to tray (1) of absorption tower and re-boiler heat duty of stripping tower are chosen as manipulated variables (inputs), while CO_2 mole fraction in absorption tower vapor product, H_2O mole fraction in absorption tower liquid product and tray temperature No.36 of stripping tower are determined as controlled ones (outputs). The system identification is performed with three input and three output variables using the step response test. As a result, continuous and discrete-time transfer function matrices and suitable NMSS model for PIP controller are reported. Finally, to evaluate the PIP control performance, the feed flow rate increases by 2%. The results display the proper performance of the designed PIP controller for both eliminations of disturbance and tracking of set point.

Introduction

Newly, a usual approach for design control is the use of state variable feedback (SVF). It is based on a system model of the state-space formulation [1]. The state-space model indicates state variables in time-domain and model equations in a matrix form [2], in which complete SVF control is implemented directly from the measured input and output variables [3]. With the implementation of the state-space model, different types of conventional methods of SVF, including linear quadratic Gaussian (LQG), linear quadratic regulator (LQR), and pole placement can be used [4]. The main problem in the state-space approach is that the state vector can not usually be used for direct measurement [1]. Therefore, an observer is required for estimating the system's current state [3]. The use of a state observer reduces the control system robustness [1].

The PIP control, called true digital control (TDC), is a proper approach to the identification, control, and optimization of the system [5]. The PIP control design procedure had first introduced by Young and Wang. This method presents a simple solution to the problem of state vector inaccessibility for which, direct measurement by defining the NMSS formulation becomes possible [1]. Although PIP controller can be considered as a rational extension to the

* Corresponding author:
Email: sadeghi@eng.usb.ac.ir (J. Sadeghi)

conventional PI/PID controller, it is an inherent model of predictive control action, additional feedback, and input compensators, which is used for multivariable control without limitation on the number of controlled variables [6]. For first-order single-input – single-output (SISO) systems, this results in an identical method to conventional PI design [5]. The PIP controller can be revealed better than PI/PID one when the process has second-order, higher dynamics [6], or greater pure time delays than an interval sample [7]. The main positive point of this method is that the state vector consists only of those states that can be directly measured [1], without using the state observer algorithm [8]. These states are the past values of the system input and output variables and the present values of the system output variables [1]. Another advantage is that, in TDC, model identification until estimation to control is performed in digital form so that there would not be any error and digital difficulty [5]. In other words, the open-loop system identification and estimation for the linear transfer function model are carried out off-line that is followed by an on-line administration to control the operations [1].

In MIMO and higher order SISO systems, since PIP controller introduces additional filtrations and compensations as an extension for PI design, this method is easily compatible with MIMO systems for which there is no need to do modification and delay pure time consideration of the system [5]. The adjustable parameters of the PIP control method are demonstrated by the weights of the LQR cost function and the appropriate performance of closed-loop is achieved by proper adjustment of these parameters [9].

Young et al. [10] introduced NMSS and PIP controllers. Wang and Young [11] investigated the controllability of the PIP controller. Taylor et al. [12] illustrated the predictive property of the PIP controller and it is concluded that the structure of the PIP-LQ controller is similar to both general predictive control (GPC) and LQG. Young et al. [13] examined the PIP controller for SISO linear systems with delta (δ) operator models. Chotai et al. [14] inquired the PIP controller about MIMO linear systems with delta (δ) operator models.

Having made these points, ammonia is considered the most important and expensive petrochemical products. The carbon dioxide absorption unit, which is a subset of ammonia one, not only removes the harmful carbon dioxide from the catalyst in the ammonia synthesis reactor but also is an electrolytic system with strong nonlinear behavior. The chief reason why versus applied disturbances, the ammonia becomes steady for a long time is that it has slow dynamic features. It is essential to select an appropriate control structure for the CO_2 absorption unit that can perform well versus the applied disturbances and transmit the unit from a steady state to a new one with little changes. Aroua et al. [15] generated the parameters of the electrolyte NRTL model to predict the CO_2 solubility in single amine solutions (MDEA and AMP) also their binary mixtures. Rahimpour et al. [16] studied the influences of mathematical model important parameters, including amine absorbent addition and operating pressure, for the elimination of CO_2 from the synthesis gas into amine-promoted hot potash solution. Maceiras et al. [17] explored that when the amine concentration and temperature increase the volumetric mass transfer coefficient in the CO_2 absorption process rises. They presented an experiential correlation type Boltzmann to estimate the operating temperature at different gas flow rates and solvent concentrations. Mores et al. [18] modeled the reactive behavior of the CO_2 chemical absorption by an NLP mathematical model. This model is implemented in GAMS and optimized the operating conditions to maximize the CO_2 capture. Shen et al. [19] presented a rate-based dynamic model for the amine-based CO_2 absorption system. By using this model, they simulated the CO_2 absorption process control system for the treatment of the coal-fired power plant flue gas. The results showed the proper performance of the control system versus the applied disturbances.

This research aims to indicate the performance of the PIP controller in the case of MIMO and the square control structure of the carbon dioxide absorption system. The Explanation for NMSS form and its optimal control using the LQ cost function is presented in section 2. In

section 3, a brief description of the CO_2 absorption system is demonstrated and simulation of both commercial steady-state and dynamic simulators are done. In section 4, multivariable control of the CO_2 absorption system is investigated by applying the PIP control configuration to the dynamic model of the system. In section 5, the designed PIP controller performance is appraised, in which the feed flow rate is increased by 2% and the results are presented and discussed. At last, the overall conclusion of this research is exhibited in section 6.

The PIP Controller Design

Discrete-Time Transfer Function

The discrete-time transfer function model of the multi-input - multi-output (MIMO) system is shown in terms of the left matrix fraction description (LMFD) as Eq. 1.

$$y(k) = \left(A(z^{-1}) \right)^{-1} B(z^{-1}) u(k) \tag{1}$$

where $u(k)$ and $y(k)$ are the $r \times 1$ input and $p \times 1$ output vectors, respectively. z^{-1} is the backward shift operator. $A(z^{-1})$ and $B(z^{-1})$ are the transfer function polynomials [7] shown as follows:

$$A(z^{-1}) = I + A_1 z^{-1} + \ldots + A_n z^{-n} \qquad (A_n \neq 0) \tag{2}$$
$$B(z^{-1}) = B_1 z^{-1} + B_2 z^{-2} + \ldots + B_m z^{-m} \qquad (B_m \neq 0) \tag{3}$$

Here, A_i (i = 1, 2, . . ., n) are $p \times p$ and B_i (i = 1, 2, . . ., m) are $p \times r$ matrices and I is an $(p \times p)$ identity matrix [20].

Non-Minimal State Space (NMSS) Formulation

The state vector of Eq. 1 in the NMSS form is written as Eq. 4.

$$x(k) = [y(k)^T \quad \ldots \quad y(k-n+1)^T \quad u(k-1)^T \quad \cdots \quad u(k-m+1)^T \quad Z(k)^T]^T \tag{4}$$

where $x(k)$ is defined in terms of the past values of inputs and outputs, the present values of outputs, and the integral-of-error state variable between the output vector $y(k)$ and the command input vector $y_d(k)$. The integral-of-error state variable vector is defined as Eq. 5.

$$Z(k) = Z(k-1) + \left(y_d(k) - y(k) \right) \tag{5}$$

The NMSS model is written as:

$$x(k) = F x(k-1) + G u(k-1) + D y_d(k) \tag{6}$$
$$y(k) = H x(k) \tag{7}$$

where F, G, D, and H are state transition matrix, input coefficient matrix, command input coefficient matrix, and output coefficient matrix, respectively [1]. The state matrices are defined as follows:

$$F = \begin{bmatrix} -A_1 & -A_2 & \cdots & -A_{n-1} & -A_n & B_2 & B_3 & \cdots & B_{m-1} & B_m & 0 \\ I_p & 0 & \cdots & 0 & 0 & 0 & 0 & \cdots & 0 & 0 & 0 \\ 0 & I_p & \cdots & 0 & 0 & 0 & 0 & \cdots & 0 & 0 & 0 \\ \vdots & \vdots & \ddots & \vdots & \vdots & \vdots & \vdots & \ddots & \vdots & \vdots & \vdots \\ 0 & 0 & \cdots & I_p & 0 & 0 & 0 & \cdots & 0 & 0 & 0 \\ 0 & 0 & \cdots & 0 & 0 & 0 & 0 & \cdots & 0 & 0 & 0 \\ 0 & 0 & \cdots & 0 & 0 & I_r & 0 & \cdots & 0 & 0 & 0 \\ 0 & 0 & \ddots & 0 & 0 & 0 & I_r & \ddots & 0 & 0 & 0 \\ \vdots & \vdots & \cdots & \vdots & \vdots & \vdots & \vdots & \cdots & \vdots & \vdots & \vdots \\ 0 & 0 & \cdots & 0 & 0 & 0 & 0 & \cdots & I_r & 0 & 0 \\ A_1 & A_2 & & A_{n-1} & A_n & B_2 & B_3 & & B_{m-1} & B_m & I_p \end{bmatrix} \tag{8}$$

$$G = [B_1 \quad 0 \quad 0 \quad \cdots \quad 0 \quad I_r \quad 0 \quad 0 \quad \cdots \quad 0 \quad -B_1]^T \tag{9}$$

$$D = [0 \quad 0 \quad 0 \quad \cdots \quad 0 \quad 0 \quad 0 \quad 0 \quad 0 \quad \cdots \quad I_p]^T \tag{10}$$

$$H = [I_p \quad 0 \quad 0 \quad \cdots \quad 0 \quad 0 \quad 0 \quad 0 \quad 0 \quad \cdots \quad 0]^T \tag{11}$$

Here, I_p and I_r are p×p and p×r identity matrices, respectively, and 0 is a properly defined matrix of zeros [11,20].

SVF and PIP Control

The state variable feedback (SVF) control law is defined as Eq. 12.

$$u(k) = -Vx(k) \tag{12}$$

where V, called control gain matrix (CGM), is calculated by linear-quadratic (LQ) optimal control. The PIP controller algorithm is depicted in Fig. 1.

By minimizing the quadratic cost function, the LQ optimal control can calculate the CGM (V). Eq. 13 is the standard formulation of the infinite time optimal LQ servo mechanism cost function for the SISO system.

$$J = \frac{1}{2} \sum_{k=0}^{\infty} x(k)^T \, Q \, x(k) + u(k)^T \, R \, u(k) \tag{13}$$

The positive semi-definite symmetric state weighting matrix, Q, has the dimension n+m and R is a positive definite symmetric input weighting matrix. To minimize the cost function, an optimal control law is defined as Eq. 14.

$$u(k) = - \left(R + G^T PG \right)^{-1} G^T PFx(k) \tag{14}$$

P is determined by solving the following algebraic Riccati equation (ARE). The Riccati equation is depicted in Fig. 2.

$$P - F^T PF + F^T PG \left(R + G^T PG \right)^{-1} G^T P F - Q = 0 \tag{15}$$

The optimal CGM, V, is calculated from Eq. 16.

$$V = \left(R + G^T PG \right)^{-1} G^T PF \tag{16}$$

The closed-loop behavior of the system is identified by substituting Eq. 12 and Eq. 16 into Eq. 6.

$$x(k) = \left(F - G \left(R + G^T PG \right)^{-1} G^T P F \right) x(k-1) + D y_d(k) \tag{17}$$

Eigenvalues or closed-loop poles can be achieved from Eq. 18. These eigenvalues can be arbitrarily assigned in a pole assignment algorithm if and only if the pair [F, G] is controllable [20].

$$det \left\{ \lambda I - F + G \left(R + G^T PG \right)^{-1} G^T P F \right\} = 0 \qquad (18)$$

The suitable performance of closed-loop can be achieved by concurrent optimization of the diagonal LQ weights or manual tuning.

In more challenging conditions, the PIP control structure is appropriate for a combination within a multi-objective optimization outline, where acceptable agreement is achieved between opposite objectives such as multivariable decoupling, rise times, robustness, and overshoot [21].
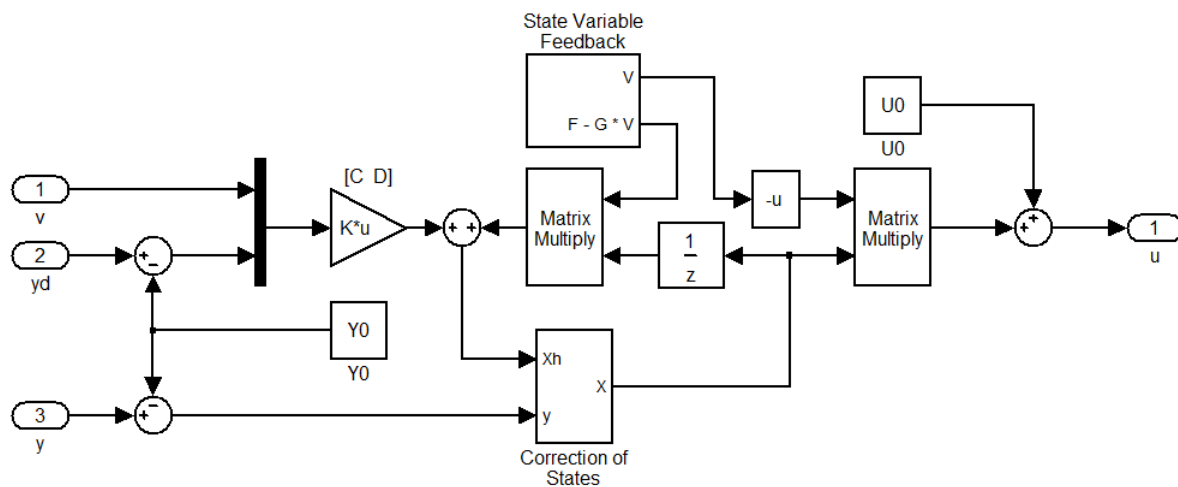

Fig. 1. PIP controller algorithm

Process Description

The carbon dioxide absorption system, which is obtained from the Shiraz petrochemical ammonia unit, has been selected as a case study. The carbon dioxide absorption system is used to remove the harmful carbon dioxide from the catalyst in the ammonia synthesis reactor. As shown in Fig. 3, the CO_2 absorption process involves one reactive absorption tower, one reactive stripping tower, one pump, one valve, and two coolers. The feed flow enters the absorption tower with a mass flow rate of 182469.4(kg/hr) containing 12.679% CO_2 mole-fraction. The phase and chemical separation are simultaneously done in two towers. The solution contains potassium carbonate and Diethanolamine (DEA), called Benfield solution, which is used for CO_2 absorption. The feed flow is contacted, counter-current, with the Benfield solution in the absorption tower where almost all of the carbon dioxide is absorbed by the forward reaction, shown in Table 1. The rich solution enters into the stripping tower, under the conditions of low pressure and high temperature, following this, carbon dioxide is removed, then the absorbent solution is regenerated by the backward reaction as is indicated in Table 1. Furthermore, one-quarter and three-quarter of the lean solution from the regenerator are cooled down and are fed to tray No.1 and tray No.14 of the absorption tower, respectively [22]. The carbon dioxide quantity in the vapor product of the absorption tower reduces to a 0.198 mole fraction. The feed, product, and equipment specifications are presented in appendix A.
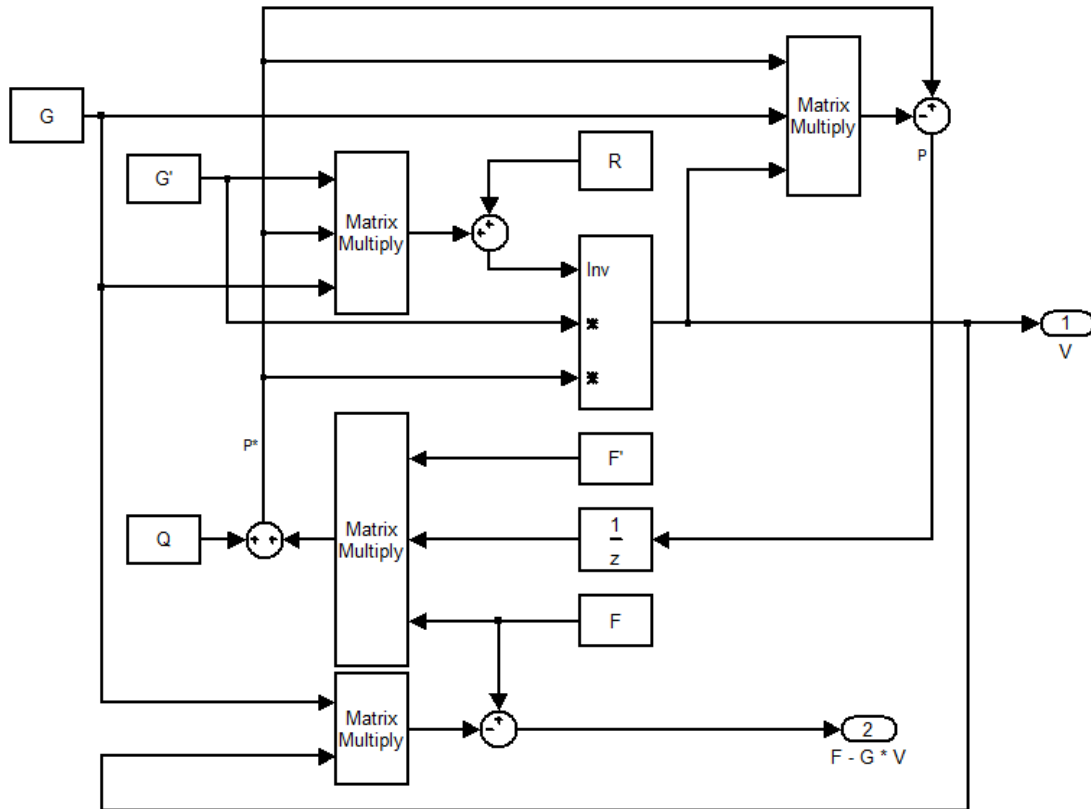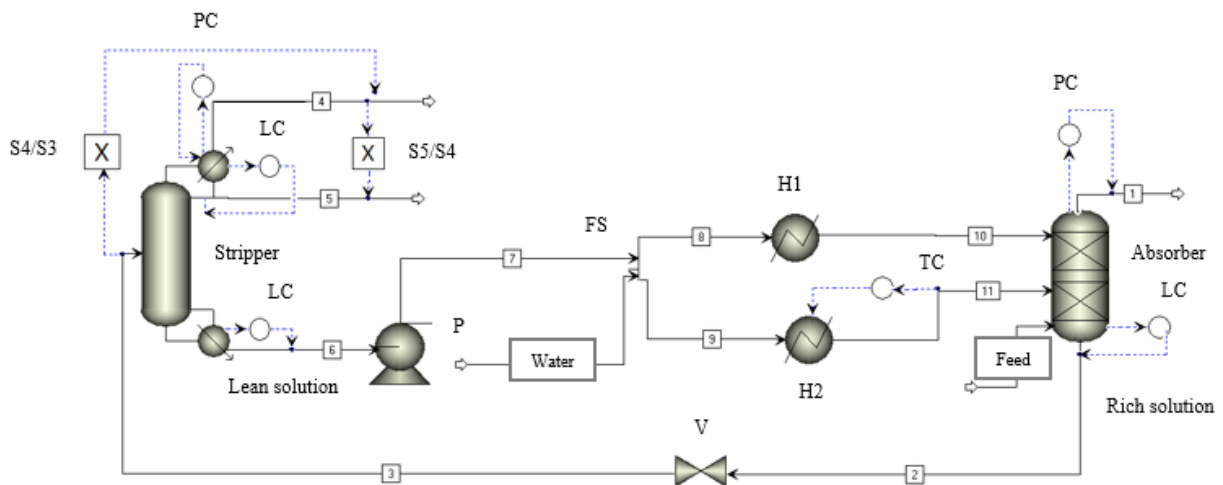
Fig. 2. Riccati equation algorithm

Fig. 3. The process flowsheet of the carbon dioxide absorption

Table 1. The equilibrium reaction of CO_2 absorption process

The CO_2 absorption process	Reaction
Absorption tower Stripping tower	$K_2CO_3 + H_2O + CO_2 \rightleftharpoons 2KHCO_3$

Process Simulation

The carbon dioxide absorption system is simulated at a steady-state using the Aspen Plus 2006.5 simulator. The type of reactive absorption and stripping towers is a packed column. The number of the equivalent equilibrium stages of towers is calculated by height equivalent to a theoretical plate (HETP) [23]. The height and volume of the filled section, the tower diameter, the assumed

value of HETP, and the number of the equivalent equilibrium stages are presented in appendix A. To simulate the chemical – phase equilibrium process in these towers, the Rad Frac model is used. To investigate the CO_2 solubility in the Benfield solution, ehotdebkp data package is used [22]. By choosing this package, the CO_2 absorption process reactions, presented in Table 2, with their kinetic constants are defined in the Chemistry sheet from the Reaction folder. The CO_2 absorption process, because of the presence of the electrolytic and polar solvent of K_2CO_3, is an aqueous electrolyte system. The ELECNRTL state equation is appropriate to compute the activity coefficients of ions and molecules in solution. In the CO_2 absorption process, the Diethanolamine absorbent amount removed from the absorption tower vapor product is small. Therefore, the same amount of Diethanolamine is injected into the loop of this process. To verify the steady-state simulation results, vapor product design data of the absorption tower are compared with the simulation results, which are shown in appendix A. The design data are accessible to the process flow diagram (PFD) of the Shiraz petrochemical ammonia unit.

To simulate the process in the dynamic state, the height and diameter of the sump and reflux drum and the hydraulic trays of two towers are defined in a dynamic sheet of equipment. Then, the Aspen Plus is exported to Aspen dynamic. The dynamic simulation of the CO_2 absorption process is done by flow driven procedure and mathematical method of Implicit Euler integral. The Aspen Dynamic put the default pressure and level controllers to towers, which are related to the process stability. In the stripping tower, two multipliers are used to control the vapor product flow rate ratio of the tower to the tower feed flow rate and two product flow rates ratio of the tower top. Also, to maintain the temperature profile constantly in the absorption tower, the cooler heat duty is applied to control the temperature of the input absorbent flow to tray No.14 of the absorption tower. In Fig. 3, the control loops of the CO_2 absorption system are indicated.

Table 2. The chemical reactions of the CO_2 absorption process

Process equipment	Chemistry reactions
Absorption tower	$DEA^+ + H_2O \rightleftharpoons DEA + H_3O^+$
Stripping tower	$CO_2 + 2H_2O \rightleftharpoons H_3O^+ + HCO_3^-$
Valve (one number)	$HCO^{3-} + H_2O \rightleftharpoons H_3O^+ + CO_3^{2-}$
Pump (one number)	$DEACOO^- + H_2O \rightleftharpoons DEA + HCO_3^-$
Cooler (two numbers)	$2H_2O \rightleftharpoons H_3O^+ + OH^-$
	$K_2CO_3 \rightarrow 2K^+ + CO_3^{2-}$
	$KHCO_3 \rightarrow K^+ + HCO_3^-$

Multivariable Control of CO_2 Absorption Process

Control structure means selecting the appropriate manipulated and controlled variables. The appropriate control structure can reject disturbances arising from setpoint changes.

Manipulated Variables

To determine the manipulated variables, product quality control variables in the Aspen Dynamic simulator are used. The carbon dioxide absorption unit consists of the reactive absorption towers, reactive stripping ones, and two heat exchangers. The degrees of freedom in absorption tower, stripping one with three outputs and heat exchangers are 2, 6, 1, and 1, respectively. In the absorption tower, the vapor product flow rate and the liquid product one are employed to control the pressure and the tower level, in turn. In the stripping tower, the reflux flow rate, the condenser heat duty, and the vapor product flow rate are exerted to control the reflux drum level, the tower pressure, and the ratio of the tower vapor product flow rate to the tower feed flow rate, while the tower top liquid product flow rate and the tower bottom one are utilized to oversee the ratio of the tower top two product flow rates and the sump level. Furthermore, to maintain the temperature profile constantly in the absorption tower, the cooler

heat duty is applied to control the temperature of the input absorbent flow to tray No.14 of the absorption tower. So, the re-boiler heat duty and the cooler one of the absorbent input to tray No.1 in the absorption tower are known as two remaining variables. Unlike these variables, the input water flow rate into the CO_2 absorption unit loop is characterized as one of the manipulated ones. The manipulated variables are presented in Table 3.

Table 3. Input variables

Variable	Description	Initial value	Unit
u_1	Input water flow rate	160.715	kmol/hr
u_2	Heat duty of cooler	-40.2679	GJ/hr
u_3	Reboiler heat duty	6983.14	GJ/hr

Controlled Variables

The main objective control of the carbon dioxide absorption process is maintaining the absorbed CO_2 concentration. The high cost of both installation and maintenance of the concentration controllers and the high time delay of concentration control loop compared to temperature control loop (approximately three times) lead to controlling indirectly of the concentration by temperature. As it can be seen a change in tower temperature causes a change in the concentration of the key product components. Thus, the temperature of tray No.36 of the stripping tower, as one of the controllable variables, is applied to control the CO_2 concentration in the vapor production of the stripping tower. Tray No.36 is selected based on the slope criterion [22]. For the following, the absorption tower enters vapor product into the Methanation reactor. In such a reactor, CO_2 reacts with H_2 to generate CH_4 and H_2O. The methanation reactor is a reactor in which the CO_2 concentration is employed as feed, so this needs to be preserved in such a way that the ratio of hydrogen to nitrogen in the reactor product remains constant within the specified range. Moreover, the water concentration in the reactor feed needs to exist in such an amount so that no backward reaction takes place. For this reason, CO_2 mole fraction and H_2O one of vapor and liquid product, respectively, in absorption tower are the other controlled variables, which are presented in Table 4.

Table 4. Output variables

Variable	Description	Setpoint	Unit
y_1	CO_2 mole fraction	0.002	kmol/kmol
y_2	H_2O mole fraction	0.812	kmol/kmol
y_3	Temperature of tray No.36 of stripping tower	146.347	°C

Identification of NMSS-PIP System and Structure

To identify the carbon dioxide absorption system, using the PIDIncr controller, the features of Aspen Dynamic software are considered and the first-order transfer function is assumed. The step response tests were done between each pair of input and output variables in the Aspen Dynamic simulation. Moreover, the open-loop gain, time constant, and time delay are obtained from two changes of +3% and -3% in the initial values of the input variables. To calculate the transfer function between each pair of input and output variables, the mean of open-loop gains and the mean of time constants, are achieved in two-step responses. Therefore, the matrix of the continuous transfer function is achieved as a 3-by-3 matrix. Thereupon, as described in appendix B, the continuous transfer function is transformed to LMFD for employing in the NMSS-PIP structure. The calculated state matrices (F, G, D, and H) for the CO_2 absorption system are presented in appendix B. Then, as shown in Fig. 4, by linking the Matlab-Simulink to the Aspen Dynamic model, the PIP control structure is applied to the CO_2 absorption system. For this purpose, a block called AMSimulation is added to the Simulink Library environment.

This block is an intermediary between the selected input and output variables in both Matlab-Simulink and Aspen Dynamic. The outputs of the AMSimulation block are the selected output variables, which enter the PIP controller. The controller outputs are the selected input variables. Thus, using NMSS-PIP control in Matlab-Simulink, the closed-loop simulation is examined.
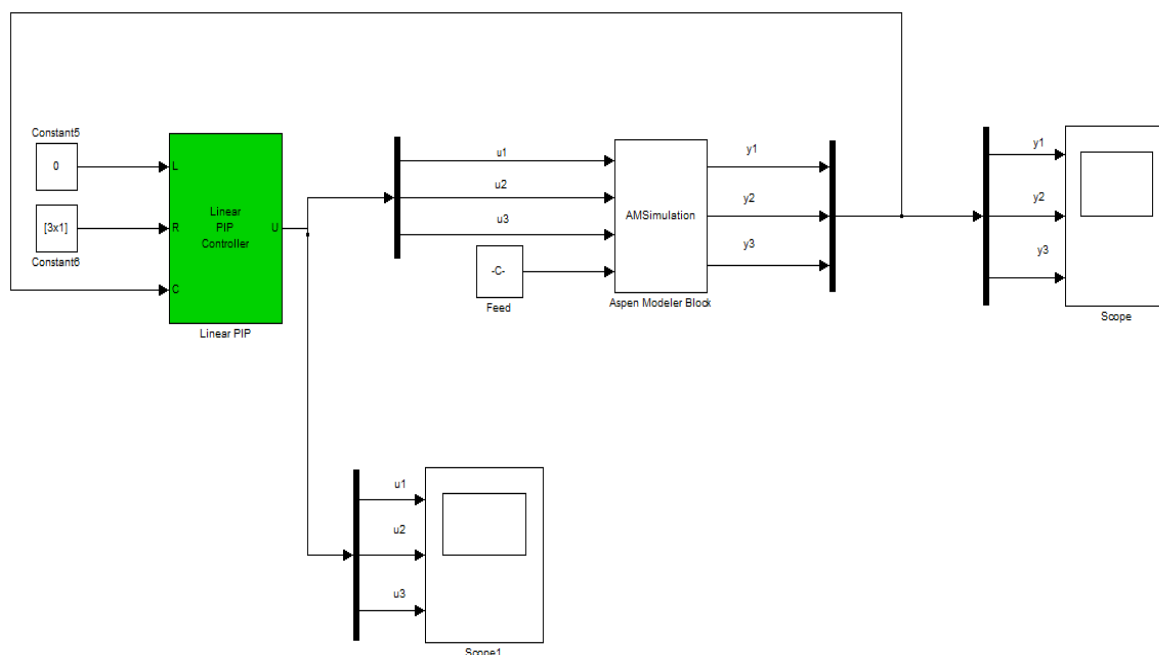

Fig. 4. PIP control in MATLAB-Simulink

Results and Discussion

To investigate the PIP control structure performance of the CO_2 absorption process, the feed flow rate increased by 2%. The PIP control appropriate performance is probable through adequate adjustments of Q (matrix of state weightings) and R (matrix of input weightings) matrices diagonal elements. In this paper, the manual adjustments of weighting matrices are carried out by trial and error method. The weighting matrices are presented in Table 5.
As shown in Figs. 5 to 10, the PIP controller has appropriate performance versus a 2% feed increase.

Table 5. matrices of state and input weightings (Q and R)

Weighting matrix	
Q	$\begin{bmatrix} 9.12e\text{-}7 & 0 & 0 & 0 & 0 & 0 \\ 0 & 3.46e\text{-}7 & 0 & 0 & 0 & 0 \\ 0 & 0 & 1.06e\text{-}11 & 0 & 0 & 0 \\ 0 & 0 & 0 & 1 & 0 & 0 \\ 0 & 0 & 0 & 0 & 1 & 0 \\ 0 & 0 & 0 & 0 & 0 & 1 \end{bmatrix}$
R	$\begin{bmatrix} 2.17e\text{-}4 & 0 & 0 \\ 0 & 0.0222 & 0 \\ 0 & 0 & 8.57e\text{-}7 \end{bmatrix}$

The carbon dioxide mole fraction changes in absorption tower vapor product are indicated in Fig. 5. The immediate rise from the carbon dioxide mole fraction in the absorption tower vapor product can be justified according to the increase in the feed flow rate. Owning the fact that in the constant amount of initially absorbent solution, the absorption operation does not

perform entirely, which results in the occurrence of this instant increase. The subsequent changes during disturbance can be attributed to the effects of three input variables simultaneous changes, which are manipulated, on the amount of carbon dioxide absorption. By itself, when the input water flow rate increases, both input absorbent cooler heat duty to tray (1) of absorption tower and re-boiler heat duty decline. This causes an increase in the absorption operation, while the CO_2 mole fraction reduces in the vapor product of the absorption tower. On the contrary, in the PIP control structure, three input variables' simultaneous changes affect the absorption rate. So at first, the input water flow rate enhances, the cooler heat duty and the re-boiler one declines. Also, the carbon dioxide mole fraction increases at a slight slope for 1.5 hours. The simultaneous changes of three input variables lead to an increase or decrease in carbon dioxide absorption rate, which causes either a decrease or increase in its mole fraction of the vapor product. As a result, three input variables change so that the carbon dioxide mole fraction returns to its setpoint after 18 hours with slight fluctuations.
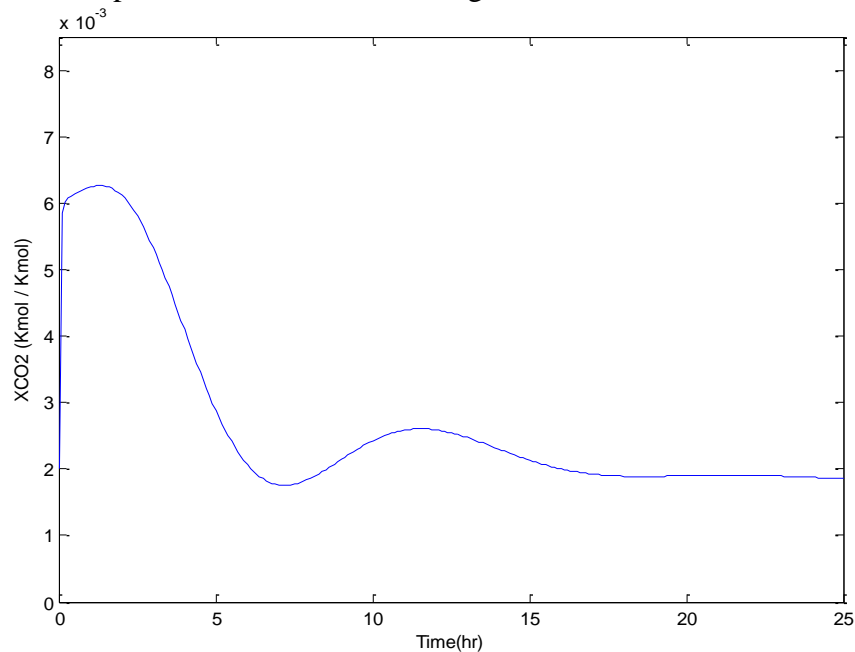

Fig. 5. CO_2 mole fraction changes in absorption tower vapor product

The water mole fraction changes in absorption tower liquid product are indicated in Fig. 6. These changes can be explained that while the feed increase, the absorption rate reduces, and thereby the water mole fraction decreases in the liquid product. After 1.5 hours, since the absorption rate increase, the water mole fraction rises as well, however, due to fluctuations in absorption rate, the water mole fraction fluctuates slightly and returns to its setpoint.

The appropriate performance of the PIP controller versus control tray temperature No.36 of the stripping tower is shown in Fig. 7. Therefore, little changes in tray temperature mean that with both increasing feed and decreasing absorption operation, the stripping tower feeds temperature declines. So the feed temperature reduction not only causes an instant decrease of tray temperature No.36 of the stripping tower but also fluidizes some vapor inside this tower. To enhance the vapor rate, the re-boiler heat duty rises, followed by an increase in the tray temperature No.36. Tray temperature No.36 of the stripping tower is more affected by re-boiler heat duty than two other input variables. It can be concluded that the system is identified by an open-loop test. The tray temperature No.36 returns to its set point with little changes (less than 0.1) when the re-boiler heat duty fluctuates.
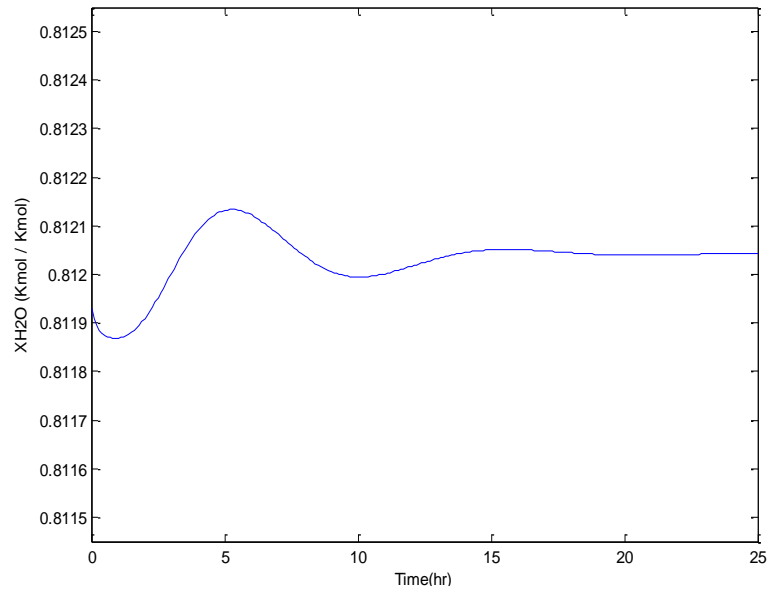
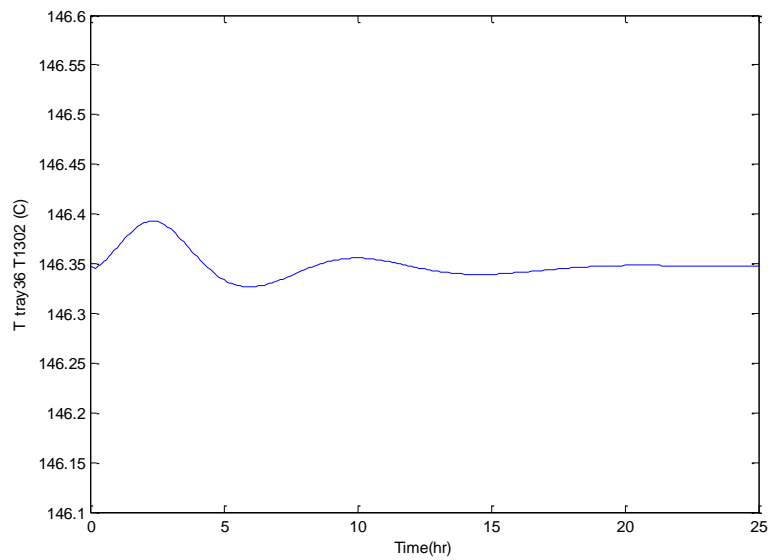**Fig. 6.** Water mole fraction changes in absorption tower liquid product

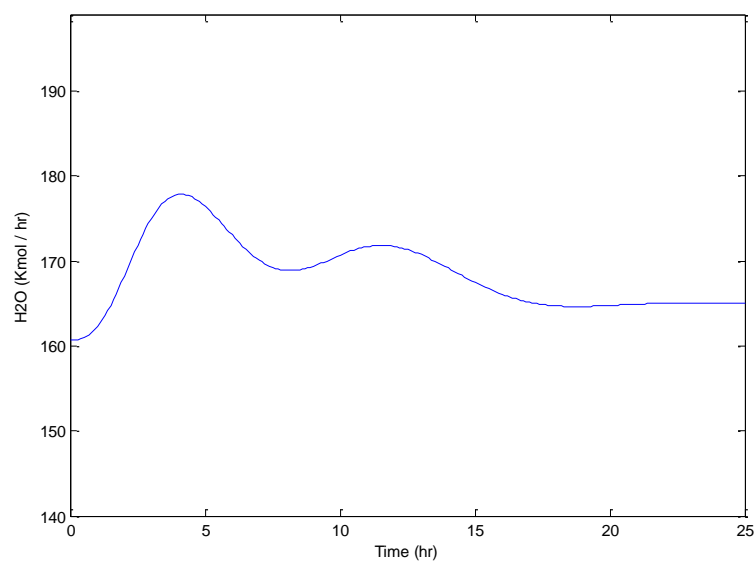**Fig. 7.** Tray temperature changes No.36 of stripping tower

Fig. 8. Input water flow rate changes to carbon dioxide absorption loop

As shown in Fig. 8, the input water flow rate increases after the disturbance are applied and it reaches a new steady value. For that purpose, an increase in more feed of absorbent solution is needed, which by enhancing the input water rate, the absorbent solution rises.

According to Fig. 9, the input absorbent cooler heat duty to tray No.1 of the absorption tower declines, because the absorbent solution increases. So to decrease the input absorbent solution temperature in the absorption tower, the cooler should be taken more heat from the absorbent solution, which generally results in a decrease in the heat duty of the cooler.
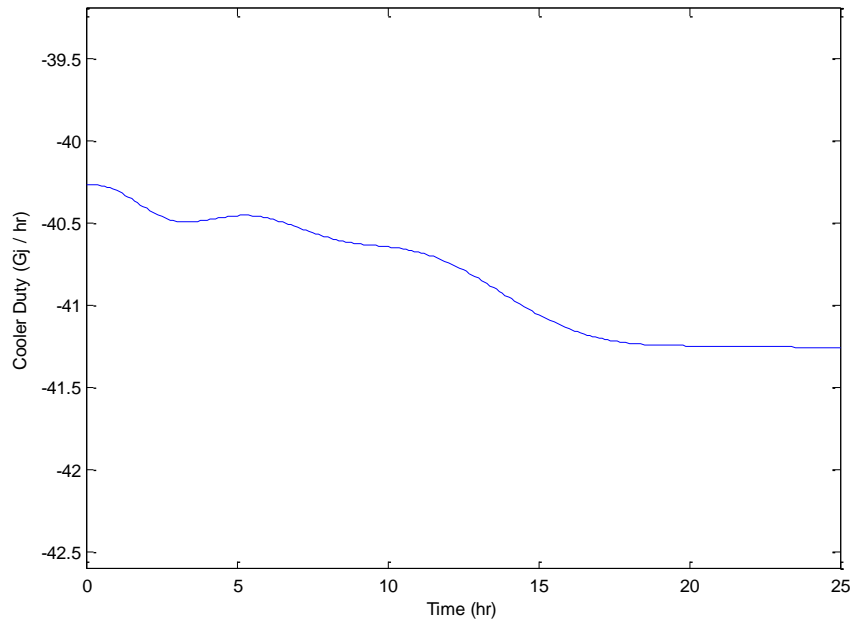

Fig. 9. Heat duty changes of input absorbent cooler to tray No.1 of absorption tower

Fig. 10 shows the reboiler heat duty changes of the stripping tower. The reboiler heat duty changes were described in section Fig. 7.

The centralized PIP controller removes the interaction between control loops and eliminates the oscillations, because of the inherent decoupler in the PIP structure and the centralized control scheme. Therefore, the results show the proper performance of the designed PIP controller for the disturbance elimination, tracking of setpoint, and improvement of process dynamic behavior. The PIP controller provides more robust control over output performances.
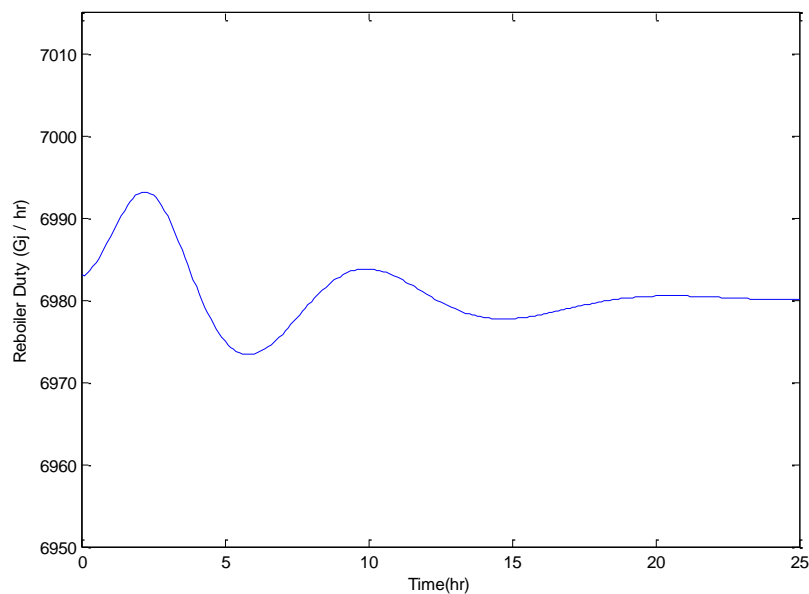

Fig. 10. Re-boiler heat duty changes of stripping tower

Conclusion

In this study, multivariable control of carbon dioxide absorption system, which is obtained from Shiraz petrochemical ammonia unit, is done using the PIP control algorithm. Therefore, a MIMO model is acquired for this system using a step response test. In the subsequent stage, a suitable NMSS model for the PIP controller is achieved. Then, a conventional method to form discrete Riccati algebraic equation is found detecting the optimal feedback gain matrix. Finally, the weighting matrices of the PIP control (Q, R) are acquired by the trial and error method. The results indicate the suitable performance of the designed PIP controller for multivariable control of the investigated unit with nonlinear behavior. The result showed that, after a 2% increase in the feed flow rate unit, the controller worked properly and prevented severe changes in the controlled variables. The PIP controller eliminated these small oscillations during 18 hours by smooth manipulation of input variables and controlled ones to return to their setpoints without severe oscillations. Having errors in the designed controller is inevitable due to manual adjustments of the diagonal elements of Q and R matrices. The captured Q and R can be used as initial guesses to determine the optimal weighting matrices of the PIP control by minimizing the error integral criteria such as ITAE, IAE, and ISE. The PIP control strategy has been done without any limitations to the structure and the order of the model. It should be noticed that there is no need for normal special techniques for MIMO process control such as decoupling. To conclude, the PIP controller provides more robust control over output performances and can be used for any system with every model order.

Nomenclature

Symbols

$A(z^{-1})$	LMFD Denominator matrix polynomial
$B(z^{-1})$	LMFD Numerator matrix polynomial
D	NMSS command input coefficient matrix
F	NMSS State transition matrix
G	Input coefficient matrix of NMSS
H	Output coefficient matrix of NMSS
I	Identity matrix
J	LQ cost function
k	Open-loop gain
K	Matrix of integral gains
Q	Matrix of state weightings
R	Matrix of input weightings
u	Vector of inputs
u	Input variable
V	Control gain matrix
x	Vector of states
y	Vector of outputs
y	Output variable
y_d	Command input vector
z^{-1}	Backward shift operator
Z	Integral-of-error state variable vector

References

[1] Nada AA, Shaban EM. The Development of Proportional-Integral-Plus Control Using Field Programmable Gate Array Technology Applied to Mechatronics System. American Journal of Research Communication. 2014;2(4):14-27.

[2] Chau, P. C., Chemical Process Control, University of California, San Diego, 2001.

[3] Zhang D, Cross P, Ma X, Li W. Improved control of individual blade pitch for wind turbines. Sensors and Actuators A: Physical. 2013 Aug 15;198:8-14.

[4] Wang L, Garnier H, editors. System identification, environmental modelling, and control system design. Springer Science & Business Media; 2011 Oct 20.

[5] Jamali P, Sadeghi J, Tavakoli S, Khosravi MA. Weight optimal Proportional-Integral-Plus control of a gasoline engine model. In2015 European Control Conference (ECC) 2015 Jul 15 (pp. 1426-1431). IEEE.

[6] Balaji V. Study and analysis of advanced control algorithms on a FOPDT model. Research Journal of Applied Sciences. 2014;9(6):376-81.

[7] Shaban EM, Nada AA. Proportional Integral Derivative versus Proportional Integral plus Control Applied to Mobile Robotic System. Journal of American Science. 2013;9(12):583-91.

[8] Shaban EM. Deadbeat response of nonlinear systems described by discrete-time state dependent parameter using exact linearization by local coordinate transformation. Journal of American Science. 2012;8(10):355-66.

[9] Abdelhamid A, Shaban EM, Zied KM, Khalil Y. Implementation of a Class of True Digital Control (TDC) in the Navigation of a Ground Vehicle. American Journal of Research Communication. 2013;1(6):99-111.

[10] Young P, Behzadi MA, Wang CL, Chotai A. Direct digital and adaptive control by input-output state variable feedback pole assignment. International Journal of Control. 1987 Dec 1;46(6):1867-81.

[11] WANG CL, Young PC. Direct digital control by input-output, state variable feedback: theoretical background. International Journal of Control. 1988 Jan 1;47(1):97-109.

[12] Taylor CJ, Young PC, Chotai A, Dixon R. Structural and predictive aspects of proportional-integral-plus (PIP) control.

[13] Young P, Chotai A, Mckenna P, Tych W. Proportional-integral-plus (PIP) design for delta (delta) operator systems Part 1. SISO systems. International Journal of Control. 1998 Jan 1;70(1):123-47.

[14] Chotai A, Young P, McKenna P, Tych W. Proportional-integral-plus (PIP) design for delta (delta) operator systems Part 2. MIMO systems. International Journal of Control. 1998 Jan 1;70(1):149-68.

[15] Aroua MK, Haji-Sulaiman MZ, Ramasamy K. Modelling of carbon dioxide absorption in aqueous solutions of AMP and MDEA and their blends using Aspenplus. Separation and purification technology. 2002 Nov 1;29(2):153-62.

[16] Rahimpour M. R., Kashkooli A. Z., Modeling and simulation of industrial carbon dioxide absorber using amine-promoted potash solution, Iranian Journal of Science & Technology, Vol. 28, No. B6, pp. 653-666, 2004.

[17] Maceiras R, Alvarez E, Cancela MA. Effect of temperature on carbon dioxide absorption in monoethanolamine solutions. Chemical Engineering Journal. 2008 May 1;138(1-3):295-300.

[18] Mores P, Scenna N, Mussati S. Mathematical Model of Carbon Dioxide Absorption into Mixed Aqueous Solutions. InComputer Aided Chemical Engineering 2009 Jan 1 (Vol. 27, pp. 1113-1118). Elsevier.

[19] Shen MT, Chen YH, Chang H. Simulation of the Dynamics and Control Responses of the Carbon Dioxide Chemical Absorption Process using Aspen Custom Modeler. Energy Procedia. 2019 Feb 1;158:4915-20.

[20] Taylor CJ, Young PC, Chotai A. True digital control: statistical modelling and non-minimal state space design. John Wiley & Sons; 2013 May 29.

[21] Taylor CJ, Leigh P, Price L, Young PC, Vranken E, Berckmans D. Proportional-integral-plus (PIP) control of ventilation rate in agricultural buildings. Control Engineering Practice. 2004 Feb 1;12(2):225-33.

[22] Tavakoli Dastjerd F, Sadeghi J. The Simulation and Control of Ammonia Unit of Shiraz Petrochemical Complex, Iran. Journal of Chemical and Petroleum Engineering. 2018 Dec 1;52(2):107-22.

[23] Seader, J. D., Henley, E. J. and Ropert, D. K., Separation process principles. 3^{td}. Ed. Chapter 6, John Wiley & Sons, Inc Pub., United States of America, 2010.

Appendix A

<div align="center">Table A1. Feed and product specifications</div>

Parameter	Feed Flow	Absorber Vapor Product (1)	Stripper Vapor Product (4)
Temperature (°C)	115	68	35
Pressure (kg/cm^{2}g)	28.15	28	0.6
Mole Flow Rate (kgmol/hr)	11443.508	6577.962	1447.632
Mass Flow Rate (kg/hr)	182469.4	57531	63384.6
Mole Fraction			
CH_4	0.139	0.241	0.002
CO	0.278	0.483	0.003
CO_2	12.679	0.198	99.326
H_2	42.507	73.838	0.504
N_2	13.741	23.869	0.163
Ar	0.165	0.287	0.002
H_2O	30.491	1.085	-

<div align="center">Table A2. Equipment specification</div>

Equipment	Specification			
	The type of packed components	HETP(m)	The height of the filled section (m)	Number of trays
Absorber	103m^3 37mm Mini Ring S.S in 2 equal beds, 3100mm diameter 216.4m^3 50mm Mini Ring S.S in 2 equal beds, 4500mm diameter	0.6	27.25	42
Stripper	519m^3 of 50mm Mini Ring S.S in 3 equal beds, 5500mm diameter	0.6	21.84	39
Cooler (H1)	16.95 ×10^6 kcal/hr			
Cooler (H2)	41.11 ×10^6 kcal/hr			
Pump (P)	715 m3/hr , 926(kw)			

Table A3. Comparison of the absorption tower vapor product design data and the steady state simulation results

Parameter	Design data	Steady state simulation results	Relative error percentage
Temperature (ºC)	68	100.15	-47.28
Pressure (kg/cm^{2}g)	28	28	0
CH_4	0.241	0.2	-
CO	0.483	0.5	-
CO_2	0.198	0.3	-
H_2	73.838	72.4	0.019
N_2	23.869	23.4	0.020
Ar	0.287	0.3	-
H_2O	1.085	3	-

Appendix B

The transfer function between input and output variables is important at enough large times; therefore, the final value theorem is used.

$$\lim_{t \to \infty} g(t) = \lim_{s \to 0} s\ g(s) \tag{B.1}$$

The first order transfer function is as follows:

$$g_{ij} = \frac{k_{ij}}{\tau_{ij} s + 1} \approx k_{ij}\left(1 - \tau_{ij}\ s\right) = k_{ij} - k_{ij}\ \tau_{ij}\ s \tag{B.2}$$

$$\begin{bmatrix} y_1 \\ \vdots \\ y_i \end{bmatrix} = \left(\begin{bmatrix} k_{11} & \cdots & k_{1j} \\ \vdots & \ddots & \vdots \\ k_{i1} & \cdots & k_{ij} \end{bmatrix} - \begin{bmatrix} k_{11}\tau_{11} & \cdots & k_{1j}\tau_{1j} \\ \vdots & \ddots & \vdots \\ k_{i1}\tau_{i1} & \cdots & k_{ij}\tau_{ij} \end{bmatrix} s \right) \times \begin{bmatrix} u_1 \\ \vdots \\ u_j \end{bmatrix} \tag{B.3}$$

$$Y \approx (K_1 - K_2\ s)U \tag{B.4}$$

The first order transfer function matrix:

$$G = \frac{Y}{U} = \frac{K_1}{I + As} \approx (I - As)\ K_1 \tag{B.5}$$

Comparing with Eq. B.4:

$$K_2 = A\ K_1 \to A = K_2\ K_1^{-1} \tag{B.6}$$

Assuming the sample time T_s:

$$s = \frac{1 - Z^{-1}}{T_s} \tag{B.7}$$

$$z^{-1} = \frac{Y_{k-1}}{Y_k} \tag{B.8}$$

$$Y\ (I + As) = K_1\ U \tag{B.9}$$

$$Y_{k-1} + A\left(\frac{Y_k - Y_{k-1}}{T_s}\right) = K_1 U_{k-1} \tag{B.10}$$

$$Y_k = \left(-T_s\ A^{-1} + I\right) Y_{k-1} + T_s\ A^{-1}\ K_1\ U_{k-1} \tag{B.11}$$

Based on Eq. 1:

$$A_1 = -I + T_s\ A^{-1} \tag{B.12}$$

$$B_1 = T_s\ A^{-1}\ K_1 \tag{B.13}$$

Non-minimal state space model:

$$F = \begin{bmatrix} -A_1 & 0 \\ A_1 & I_p \end{bmatrix} \tag{B.14}$$

$$G = \begin{bmatrix} B_1 \\ -B_1 \end{bmatrix} \tag{B.15}$$

$$D = \begin{bmatrix} 0 \\ I_p \end{bmatrix} \tag{B.16}$$

$$H = [\ I_p \quad 0] \tag{B.17}$$

The non-minimal state space model of the CO2 absorption unit becomes:

Table B1. Left matrix fraction description (LMFD) form

State matrix

F

$$\begin{bmatrix} 1.0571 & 0.5580 & 0.0015 & 0 & 0 & 0 \\ -0.0120 & 0.6295 & 0.0001 & 0 & 0 & 0 \\ 12.9826 & 399.4476 & -0.0860 & 0 & 0 & 0 \\ -1.0571 & -0.5580 & -0.0015 & 1 & 0 & 0 \\ 0.0120 & -0.6295 & -0.0001 & 0 & 1 & 0 \\ -12.9826 & -399.4476 & 0.0860 & 0 & 0 & 1 \end{bmatrix}$$

G

$$\begin{bmatrix} -0.0001 & 0.0003 & 0 \\ 0.0001 & -0.0002 & 0 \\ -0.0594 & 0.1760 & 0.0064 \\ 0.0001 & -0.0003 & 0 \\ -0.0001 & 0.0002 & 0 \\ 0.0594 & -0.1760 & -0.0064 \end{bmatrix}$$

D

$$\begin{bmatrix} 0 & 0 & 0 \\ 0 & 0 & 0 \\ 0 & 0 & 0 \\ 1 & 0 & 0 \\ 0 & 1 & 0 \\ 0 & 0 & 1 \end{bmatrix}$$

H

$$\begin{bmatrix} 1 & 0 & 0 & 0 & 0 & 0 \\ 0 & 1 & 0 & 0 & 0 & 0 \\ 0 & 0 & 1 & 0 & 0 & 0 \end{bmatrix}$$